

## Modelling the Effects of Curtains on Water Quality of a Eutrophic Reservoir

By D.G. Nimal Priyantha\*, Takashi Asaeda\*\*,  
Satoki Saitoh\*\*\*, and Kohichi Gotoh\*\*\*

T-Dam Reservoir, one of the reservoir in Kyushu, Japan has been supplying water for paddy field irrigation. During recent years it has shown serious deterioration of water quality specially in summer. Destruction of thermocline has been prohibited to maintain desirable temperature downstream of the reservoir for paddy field irrigation. As one of the ways of reducing algal blooming in the reservoir, two vertical curtains, having depths to cover the epilimnion thickness, are installed across the reservoir in order to curtail the nutrient supply from nutrient-rich inflow to the downstream epilimnion of the reservoir. Withdrawal level is also regulated to keep the downstream epilimnion off the nutrient supply. The results of this study illustrate the consequences of curtains on algal blooming in the reservoir. The processes in the reservoir ecosystem have been modeled, by assuming stratified layered structure at each zone of the reservoir, to predict the water quality and algal species composition in the reservoir.

*Keywords:* Curtain; Entrainment; Epilimnion; eutrophication; Reservoir; Riverine

### 1. Introduction

During recent years, concern on lake and reservoir eutrophication has largely been increased in Japan. T-Dam Reservoir, one of the largest reservoirs in Kyushu, Japan has shown a serious deterioration of water quality, caused by cultural eutrophication, specially during summer time. Eutrophication process accompanied by excessive phytoplankton blooms are responsible for the characteristic greenish color, reduced transparency, and hypolimnetic oxygen depletion of the reservoir water and thus certainly impairs the recreational use of the reservoir. One of the important roles of T-Dam Reservoir is to supply water to paddy fields in the region. Paddy field irrigation requires water warmer than 17 °C. Thus, there are various drawbacks for conventional existing control devices to be applied due to the destruction of the thermocline partially or completely. The reservoir outlet also works incorporating selective withdrawal device. Although various water quality parameters are considered, the most important objective is to maintain a desirable river temperature downstream of the reservoir.

As a mean of reducing entrainment of nutrient-rich inflow into the downstream epilimnion, two plastic curtains were installed across the reservoir, having depths to cover the epilimnion thickness, on 3 March 1994. The plan view of T-Dam Reservoir and the location of the curtains are shown in Fig. 1. The curtains were mounted on floating buoys to maintain constant depth of 5 m below the water surface and installed much towards the riverine zone in which most of the inflow enters into the reservoir. The most upstream curtain was placed to cut off nutrient supply from S-River and T-River and the other curtain was installed to suspend the nutrients from Small River. Asaeda et al. (1995) analysis the experimental results and Nimal et al. (1995) discuss the variation of algae with different curtain depth. This paper discusses the modelling of surface chl-*a* and temperature of T-dam reservoir after installing curtains. During early spring up to the middle of April, inflow was lighter than the water at the surface and floats over the reservoir surface (Asaeda et al., 1995). Thus, the presence of curtains prevents the direct intrusion of the high level of nutrients to the downstream. Algal concentration is higher at upstream zones. Thus, within these zones, algae consume large amount of inflow nutrients, which cause a reduced nutrient supply to the downstream zone of the reservoir. Moreover, water in the upper layers gradually settled down until the bottom of the curtain replacing newly inflow water in the upstream zone. During this process, water below the curtain bottom flows from the upstream side to the downstream side and flows up along the curtain entraining cool heavy water in the downstream zone (see Fig. 2(A)). This entrainment leads to an increase in the density of the upward flow, which increases the submergence level of nutrient-rich interflow. During late spring and summer, presence of curtain prevents the dispersion of nutrient from upstream zones to the downstream zones. It is also found that the inflow penetration level reduced close to the withdrawal level which played a major role by withdrawing nutrient rich interflow (see Fig. 2(B)). The processes in the reservoir ecosystem have been modeled, by assuming stratified layered structure at each zone of the reservoir, to predict the water quality and algal species composition in the reservoir.

\* Student member, Doctor course student, Department of Civil Engineering, Saitama University

\*\* Member, Dr. Eng., Associate Professor, Department of Civil Engineering, Saitama University.

\*\*\* Terauchi Dam Office, Water Resources Development Public Corporation of Japan.

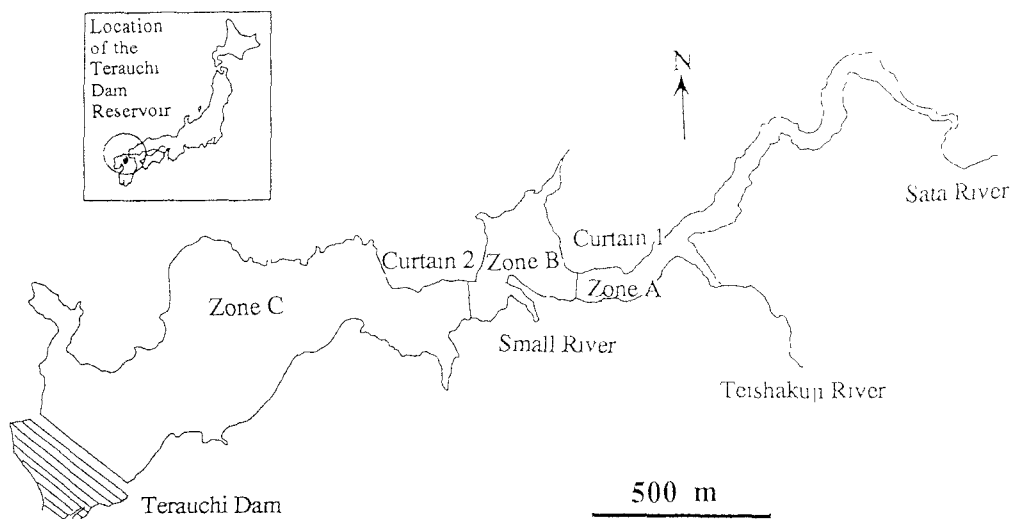


Fig. 1 Plan view of T-Dam Reservoir

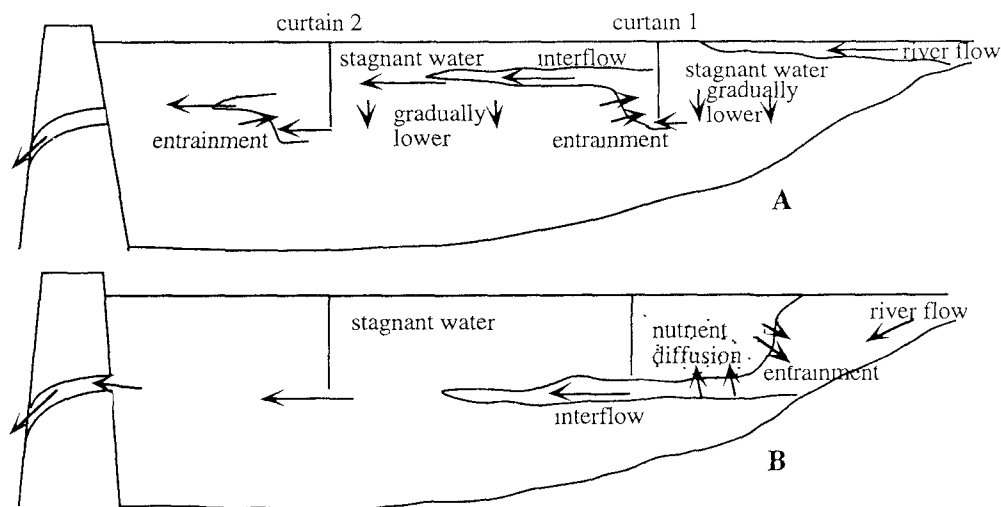


Fig. 2 Illustration of possible mechanisms after installing curtains (A) during early spring (B) during late spring and summer

## 2 Information on study site

T-Dam reservoir is located in the northern part of Kyushu, the west island of Japanese archipelago,  $33^{\circ} 25' N$  in latitude, and  $130^{\circ} 43' E$  in longitude. The reservoir is 2.5 km long, 400 m wide, 900 ha of total water surface area, and 35 m of maximum depth. Total volume of the reservoir is 18 million  $m^3$ . Three rivers enter the reservoir; the main river called S-River, enters the upstream end of the reservoir, whereas T-River and Small River enter the middle of the reservoir (Fig. 1). The Small River has the highest concentration of nutrients but its discharge is small compared with other two rivers (Saitoh and Gotoh, 1994). The morphology of the reservoir is such that it has an elongated shape as shown in Fig. 1.

## 3. Model formulations

### 3.1 Physical process sub-model

To simulate physical state variables such as temperature, one dimensional reservoir simulation model DYRESM (Imberger et al., 1978) is used after including the processes occurring due to the presence of the curtains which are identified by Asaeda et al. (1995). The DYRESM uses Lagrangian layers that expand, contract, combine, move vertically, and divided in response to the physical process within the reservoir, and

uses a one-dimensional assumption of horizontal homogeneity based on lateral and longitudinal variations in density being dissipated rapidly compared with variation caused by vertical advection. Processes included in the model are surface layer deepening, surface heat, mass and momentum exchange, mixing in the hypolimnion, inflow, and outflow. The length of a time step for each processes varies; a variable time step which is selected internally by the model based on the dynamics of surface layer for the process of surface heat transfer and wind mixing, and a fixed daily time step is used for inflow and outflow. Boundary condition at the curtains is such that there is no flow across the curtains only up to the curtain depth. Flow under the curtains from upstream side to downstream side is also considered to be insensitive to fluctuations on time scale less than one day. Flow is withdrawn under each curtain from the upstream side using the same method described in outflow dynamics in DYRESM by Imberger et al. (1978). If the withdrawal density is less than the density of the layer downstream of the curtain at the level of curtain bottom, the withdrawal water will flow up entraining reservoir water until at which its density equals that of the reservoir. This process is observed during early spring (Asaeda et al., 1995). The equations used to calculate entrainment to the upward flow are described in detail by Nimal et al. (1995). The maximum measured turbidity at the deepest part of the reservoir (Zone C) is 4.0 mg l<sup>-1</sup>. Hence, the particulate matter settling and the influence of turbidity on the light penetration are assumed to be negligible in the model formulations.

### 3.2 Ecological process sub-model

Figure 3 shows the interrelations between the state variables in the ecological sub-model which described the phytoplankton production, dissolved oxygen budget, and nutrient cycling. Vertical diffusion of biological state variables in the hypolimnion is estimated using the turbulent diffusion algorithm described by Imberger and Patterson (1981). In lake and reservoirs, phytoplankton consists of several groups. However, a group may show different ecological characteristics. Four major groups; diatoms, cyanobacteria, green algae, and flagellates are identified in T-Dam Reservoir. Hence, the model considers four phytoplankton groups. The formulations are described in detail by Nimal et al. (1995). Most of them are based on the models of MINLAKE level 3 (Riley and Stefan, 1987), and Hamilton and Schladow (1994 a).

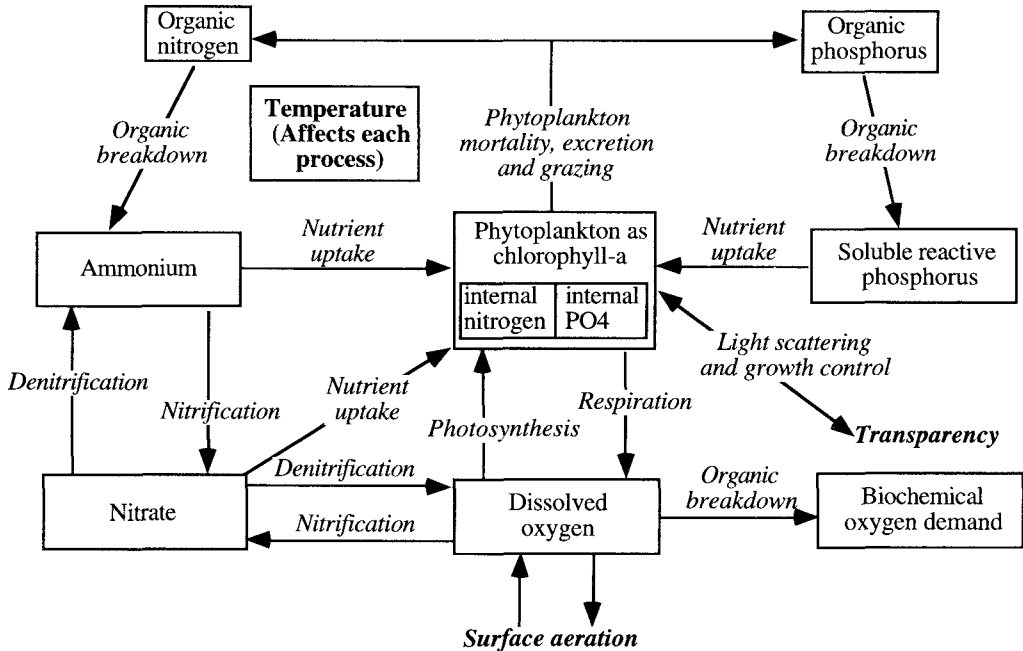


Fig. 3 Diagrammatic representation of interactions between main ecological state variables ( PO<sub>4</sub> - Phosphorus).

The state equations of the ecological sub- model are,

$$\frac{\partial P_{y_i}}{\partial t} = \left\{ G_{max} \theta_p^{T-20} \min[f(IP_i) : f(IN_i) : f(Si) : f(I)] - R_i - M_i - S_i \right\} P_{y_i} - G_{Z_i} \quad (1)$$

$$\frac{\partial IP_i}{\partial t} = U_{pmax} \theta_p^{T-20} \frac{IP_{max} - IP_i}{IP_{max} - IP_{min}} \frac{PO_4}{K_{PO_4} + PO_4} P_{y_i} - R_i IP_i - M_i IP_i - k_{gz} \theta_{gz}^{T-20} \frac{Py_i}{K_{gz} + Py_i} P_i \frac{IP_i}{Py_i} Z_p \quad (2)$$

$$\frac{\partial IN_i}{\partial t} = U_{nmax} \theta_p^{T-20} \frac{IN_{max} - IN_i}{IN_{max} - IN_{min}} f(N) P_{y_i} - R_i IN_i - M_i IN_i - k_{gz} \theta_{gz}^{T-20} \frac{Py_i}{K_{gz} + Py_i} P_i \frac{IN_i}{Py_i} Z_p \quad (3)$$

$$\begin{aligned} \frac{\partial PO_4}{\partial t} = & \sum_{i=1}^4 \left[ -U_{pmax} \theta_p^{T-20} \frac{IP_{max} - IP_i}{IP_{max} - IP_{min}} f(P) P_{y_i} + R_i IP_i + M_i (IP_i - IP_{min}) \right. \\ & \left. + k_{gz} \theta_{gz}^{T-20} \frac{Py_i}{K_{gz} + Py_i} P_i \frac{IP_i - IP_{min}}{Py_i} Z_p \right] + S_p \theta_s^{T-20} \frac{DO + K_{DO}}{DO} \frac{A_s}{V_L} + k_{op} \theta_{bod}^{T-20} Y_{p_{bod}} BOD \quad (4) \end{aligned}$$

$$\frac{\partial NO_3}{\partial t} = \sum_{i=1}^4 \left[ -U_{nmax} \theta_p^{T-20} \frac{IN_{max} - IN_i}{IN_{max} - IN_{min}} f(N) (1 - P_{NH}) P_{y_i} \right] + k_{NO} \theta_{NO}^{T-20} \frac{DO}{K_{NO} + DO} NH_4 \quad (5)$$

$$\begin{aligned} \frac{\partial NH_4}{\partial t} = & \sum_{i=1}^4 \left[ -U_{pmax} \theta_p^{T-20} \frac{IN_{max} - IN_i}{IN_{max} - IN_{min}} f(N) P_{NH} P_{y_i} + R_i IN_i + M_i (IN_i - IN_{min}) \right. \\ & \left. + k_{gz} \theta_{gz}^{T-20} \frac{Py_i}{K_{gz} + Py_i} P_i \frac{IN_i - IN_{min}}{Py_i} Z_p \right] + S_n \theta_s^{T-20} \frac{DO + K_{DO}}{DO} \frac{A_s}{V_L} \\ & - k_{NO} \theta_{NO}^{T-20} \frac{DO}{K_{NO} + DO} NH_4 + k_{on} \theta_{bod}^{T-20} Y_{n_{bod}} BOD \quad (6) \end{aligned}$$

$$\frac{\partial Si}{\partial t} = \left[ (-G_i + R_i + M_i) P_{y_i} I_{Si} + k_{gz} \theta_{gz}^{T-20} \frac{Py_i}{K_{gz} + Py_i} P_i I_{Si} Z_p \right]_{i=1} + k_{USi} \theta_{bod}^{T-20} U_{Si} \quad (7)$$

$$\frac{\partial BOD}{\partial t} = k_{BOD} \theta_{bod}^{T-20} \frac{DO}{K_{bod} + DO} BOD - \sum_{i=1}^4 k_m \theta_m^{T-20} P_{y_i} Y_{op} \quad (8)$$

$$\begin{aligned} \frac{\partial DO}{\partial t} = & W_s - W_E - k_{NO} \theta_{NO}^{T-20} \frac{DO}{K_{NO} + DO} NH_4 Y_{on} \\ & + \sum_{i=1}^4 \left\{ G_{max} \theta_p^{T-20} \min[f(P) : f(N) : f(I)] P_{y_i} Y_{op} - R_i P_{y_i} Y_{op} \right\} - k_{BOD} \theta_{bod}^{T-20} \frac{DO}{K_{bod} + DO} BOD \quad (9) \end{aligned}$$

where,  $A_s$  = area of sediment in contact with a layer ( $m^2$ );  $BOD$  = biochemical oxygen demand ( $mg\ m^{-3}$ );  $DO$  = dissolved oxygen concentration ( $mg\ m^{-3}$ );  $f(I)$  = light limiting function for growth;  $f(IN)$  = internal nitrogen limitation function for growth;  $f(IP)$  = internal phosphorus function for growth;  $f(Si)$  = silicon limitation function for growth considered only when diatoms is modelled ( $i=1$ );  $G_i$  = gross growth rate of phytoplankton ( $day^{-1}$ );  $G_{max}$  = maximum growth rate ( $day^{-1}$ );  $G_z$  = loss of phytoplankton from zooplankton grazing per day ( $mg\ m^{-3} day^{-1}$ );  $i$  = phytoplankton group, 1-diatoms, 2-green algae, 3-cyanobacteria, and 4-flagellate;  $IN$  = internal nitrogen concentration ( $mg\ m^{-3}$ );  $IN_{max}$  = maximum internal nitrogen concentration ( $mg\ m^{-3}$ );  $IN_{min}$  = minimum internal nitrogen concentration for no growth ( $mg\ m^{-3}$ );  $IP$  = internal phosphorus concentration ( $mg\ m^{-3}$ );  $IP_{max}$  = maximum internal phosphorus concentration ( $mg\ m^{-3}$ );  $IP_{min}$  = minimum internal phosphorus concentration for no growth ( $mg\ m^{-3}$ );  $IS_i$  = internal silica concentration ( $mg\ Si\ (mg\ Py_i)^{-1}$ );  $k_{BOD}$  = rate coefficient for detrial decay on dissolved oxygen ( $day^{-1}$ );  $k_{gz}$  = rate coefficient for grazing ( $day^{-1}$ );  $k_m$  = rate coefficient for mortality ( $day^{-1}$ );  $k_{NO}$  = rate coefficient for nitrification ( $day^{-1}$ );  $k_{on}$  = rate coefficient for organic decay of nitrogen ( $day^{-1}$ );  $k_{op}$  = rate coefficient for organic decay of phosphorus ( $day^{-1}$ );  $k_{USi}$  = rate coefficient for mineralisation of unreactive silica ( $day^{-1}$ );  $K_{bod}$  = half saturation constant for dependence of detrial decay on dissolved oxygen ( $mg\ m^{-3}$ );  $K_{DO}$  = factor regulating sediment nutrient release with dissolved oxygen concentration ( $mg\ m^{-3}$ );  $K_{gz}$  = half saturation constant for zooplankton grazing

( $\text{mg m}^{-3}$ );  $K_N$  = half saturation constant for nitrogen uptake ( $\text{mg m}^{-3}$ );  $K_{NO}$  = half saturation constant for dependence of nitrification or denitrification on dissolved oxygen ( $\text{mg m}^{-3}$ );  $M_i$  = natural mortality except grazing by zooplankton ( $\text{day}^{-1}$ );  $NH_4$  = concentration of ammonium ( $\text{mg m}^{-3}$ );  $NO_3$  = concentration of nitrate ( $\text{mg m}^{-3}$ );  $P_i$  = preference factor for specific phytoplankton group;  $P_{NH}$  = preferential ammonium uptake;  $PO_4$  = concentration of soluble reactive phosphorus ( $\text{mg m}^{-3}$ );  $P_{y_i}$  = phytoplankton concentration of group  $i$  ( $\text{mg m}^{-3}$ );  $R_i$  = respiration of phytoplankton ( $\text{day}^{-1}$ );  $S_i$  = reactive silica ( $\text{mg m}^{-3}$ );  $S_n$  = sediment nitrogen release rate ( $\text{mg m}^{-2}$ );  $S_p$  = sediment phosphorus release rate ( $\text{mg m}^{-2}$ );  $T$  = temperature ( $^{\circ}\text{C}$ );  $Un_{max}$  = maximum rate of nitrogen uptake ( $\text{day}^{-1}$ );  $Up_{max}$  = maximum rate of phosphorus uptake ( $\text{day}^{-1}$ );  $US_i$  = unreactive silica concentration ( $\text{mg m}^{-3}$ );  $V_L$  = maximum rate of phosphorus uptake;  $W_s$  = Oxygen flux from surface applies only when considering surface layer of depth  $\Delta z_i$  ( $\text{mg m}^{-3} \text{ day}^{-1}$ );  $WE$  = Oxygen demand in sub-euphotic zone applies only when considering sub-euphotic zone for a layer of depth  $\Delta z$  ( $\text{mg m}^{-3} \text{ day}^{-1}$ );  $Y_{nbod}$  = ratio of nitrogen release to oxygen utilized in organic decay;  $Y_{on}$  = stoichiometric ratio of oxygen to nitrogen for nitrification;  $Y_{op}$  = ratio of mass of oxygen produced or respired to mass of chlorophyll- $a$ ;  $Y_{pbod}$  = ratio of phosphorus release to oxygen utilized in organic decay;  $z$  = depth measured from water surface to a layer (m);  $Z_p$  = zooplankton concentration ( $\text{mg m}^{-3}$ );  $\Delta z$  = thickness of the layer (m);  $\mu$  = light extinction coefficient ( $\text{m}^{-1}$ );  $\mu_b$  = background light extinction coefficient ( $\text{m}^{-1}$ );  $\mu_{p_y}$  = specific light extinction coefficient for phytoplankton ( $\text{m}^2 \text{ mg}^{-1}$ );  $\theta_{gz}$  = temperature multiplier for grazing;  $\theta_m$  = temperature multiplier for mortality;  $\theta_p$  = temperature multiplier for growth;  $\theta_r$  = temperature multiplier for respiration;  $\theta_s$ ,  $\theta_b$  = temperature adjustment coefficient;  $\theta_{NO}$  = temperature multiplier for nitrification.

#### 4. Results and discussion

The temperature sub-model is independent of calibration of the ecological component of the model. Figure 4 shows the measured and simulated temperature distribution of surface layers of Zone A, Zone B, and Zone C. A fair match was observed between measured and simulated temperature distributions.

The ecological sub-model is calibrated over 115 days available data, from the beginning of March to the end of June, 1994. The model was initialized using the measurements taken on March 3. The measurement include each zone profiles of temperature, total chlorophyll- $a$ , phosphorus, nitrate nitrogen, ammonium, BOD, and silica. Values other than temperature below 6 m depth were set equal to the values measured at 6 m. Total chlorophyll- $a$  concentration was converted into each group by considering the phytoplankton counts, assuming linear relation between cell numbers and chlorophyll- $a$  for each group.

Predominant species of phytoplankton in the reservoir was *Melosira* in March, which was replaced by *Synedra* at the beginning of April. In the late April, *Phormidium* and *Cyclotella kuetzingiana* propagated instead of *Synedra*. *Fragilaria* dominated in May. However, in this paper total biomass is expressed in terms of chlorophyll- $a$  regardless of the variety of species to look into the aspects pertaining to current method on algal blooming. Parameters in the ecological model were found from Jorgensen et al. (1991) and Hamilton and Schladow (1994b). The parameter values found in literature were not necessarily as constants but as approximate values or intervals. Therefore all literature values for ecological parameters have some uncertainty. Hence the parameter values were set to give the best agreement between model output and measured state variables.

Measured and simulated total chlorophyll- $a$  concentration at the surface layer of the three zones are shown in Fig. 5. In Zone A, estimated values showed variation from some measured values. This variation could be due to several reasons. One reason is that it may be due to chlorophyll- $a$  concentration of the inflow. The inflow chlorophyll- $a$  was measured once a month, hence interpolated values between two months were used. These interpolated values might have higher deviation from their real values. Another reason could be due to the average parameter values. One parameter represents the average values of several species. As each species has its own characteristic parameters, the variation in the species composition inevitably gives a corresponding variation in the average parameter used in the model.

#### 5. Conclusion

This study has been presented a model that combines the mixing dynamics of a stratified lake with the biological processes, diffusion, and flow under the curtains. The model has been run using lake data from the T-Dam Reservoir. The ecological sub-model is calibrated over 115 days available data, from the beginning of March to the end of June, 1994. The model was initialized using the measurements taken on March 3. The measurement include each zone profiles of temperature, total chlorophyll- $a$ , phosphorus, nitrate nitrogen,

ammonium, BOD, and silica. The model simulate the temperature and chlorophyll-*a* concentration in the three zones of the reservoir with reasonable accuracy. Curtain method can mostly be applied for a reservoir or lake having an elongated shape. This method is particularly a low-cost technique with higher degree of reliability and simplicity compared to other existing control measures.

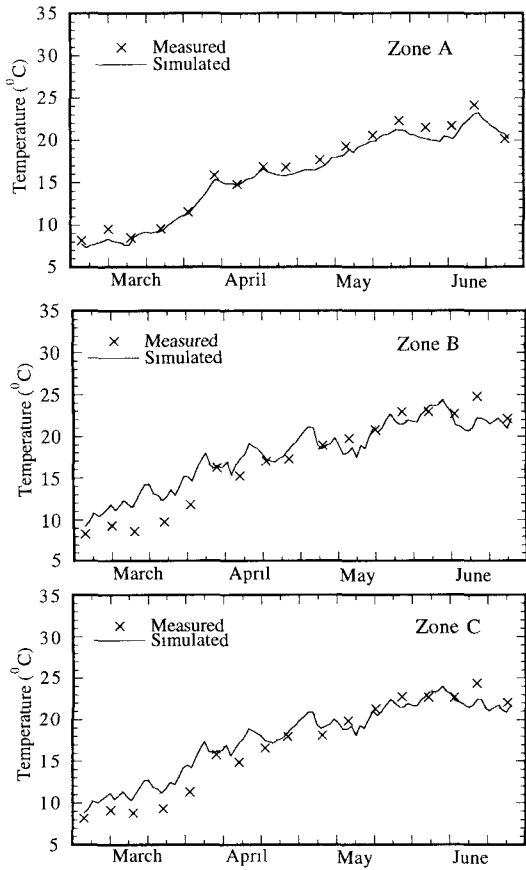


Fig. 4 Measured and simulated temperature distributions in the top layer of the three zones of T-Dam Reservoir in 1994.

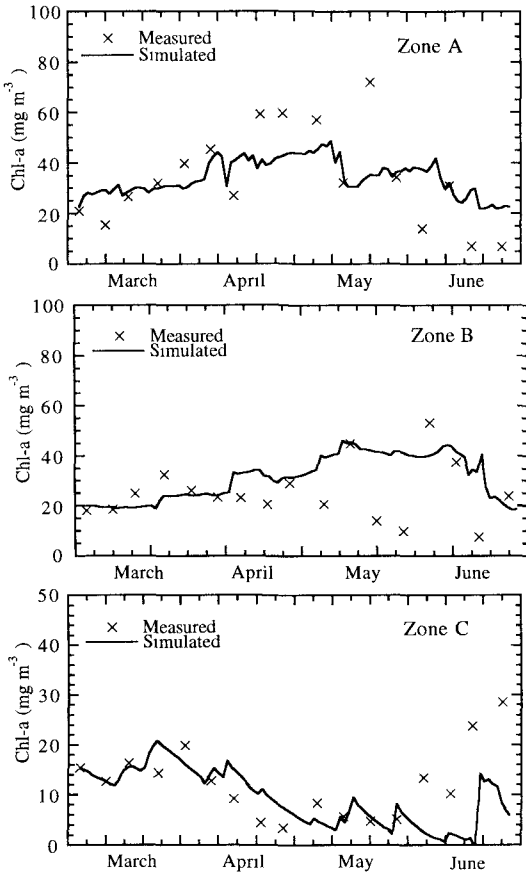


Fig. 5 Measured and simulated chlorophyll-*a* distributions in the top layer of the three zones of T-Dam Reservoir in 1994

### References

Asaeda, T., Nimal Priyantha, D.G., Saitoh, T. and Gotoh, K., 1995. A new technique for controlling algal blooming using vertical curtains in withdrawal zone of reservoirs. *Ecol. Engineering* (Submitted)

Hamilton, D.P. and Schladow, S.G., 1994a. Prediction of water quality in lakes and reservoirs: Part I: Model description. Report No. ED 597DH, Centre for Water Research, University of Western Australia, 29 pp.

Hamilton, D.P. and Schladow, S.G., 1994b. Prediction of water quality in lakes and reservoirs: Part II: Model calibration, sensitivity analysis, Verification and validation. Report No. ED 597DH, Centre for Water Research, University of Western Australia, 13 pp.

Imberger, J., Patterson, J. and Loh, I., 1978. Dynamics of reservoirs of medium size. *J. Hydr. Div , ASCE*, 104: 725-743.

Imberger, J. and Patterson, J.C., 1981. A dynamic reservoir simulation model- DYRESM 5. In: H.B. Fisher (ed.), *Transport models for inland and coastal waters*, Academic Press, N Y., 310-316.

Jorgensen, S.E., Nielsen, S.N. and Jorgensen, L.A., 1991. *Handbook of ecological parameters and ecotoxicology*. Elsevier, Amsterdam, 1264 pp.

Nimal Priyantha, D.G., Asaeda, T., Saitoh, T. and Gotoh, K., 1995. Modelling of curtain method, a new technique for controlling algal blooming in withdrawal zone of reservoirs. *Ecol. Modelling* (Submitted).

Riley, M.J. and Stefan, H.G., 1987. Dynamic lake water quality simulation model "MINLAKE". Report No. 263, St. Anthony Falls Hydr. Lab., University of Minnesota, 140 pp.

Saitoh, T. and Gotoh, K., 1994. Water management of Terauchi Reservoir (in Japanese). *Water Resources Development Public Corporation of Japan*, 19 pp.